α-Sheet secondary structure in amyloid β-peptide drives aggregation and toxicity in Alzheimer's disease

Dylan Shea[a], Cheng-Chieh Hsu[b], Timothy M. Bi[b], Natasha Paranjapye[b], Matthew Carter Childers[b], Joshua Cochran[c], Colson P. Tomberlin[d], Libo Wang[e], Daniel Paris[f], Jeffrey Zonderman[e], Gabriele Varani[c], Christopher D. Link[d], Mike Mullan[f], and Valerie Daggett[a,b,1]

[a]Department of Molecular Engineering, University of Washington, Seattle, WA 98195; [b]Department of Bioengineering, University of Washington, Seattle, WA 98195; [c]Department of Chemistry, University of Washington, Seattle, WA 98195; [d]Department of Integrative Physiology, University of Colorado, Boulder, CO 80309; [e]Redshift BioAnalytics, Burlington, MA 01803; and [f]Roskamp Institute, Sarasota, FL 34243

Edited by Angela M. Gronenborn, University of Pittsburgh School of Medicine, Pittsburgh, PA, and approved March 26, 2019 (received for review December 4, 2018)

Alzheimer's disease (AD) is characterized by the deposition of β-sheet–rich, insoluble amyloid β-peptide (Aβ) plaques; however, plaque burden is not correlated with cognitive impairment in AD patients; instead, it is correlated with the presence of toxic soluble oligomers. Here, we show, by a variety of different techniques, that these Aβ oligomers adopt a nonstandard secondary structure, termed "α-sheet." These oligomers form in the lag phase of aggregation, when Aβ-associated cytotoxicity peaks, en route to forming nontoxic β-sheet fibrils. De novo-designed α-sheet peptides specifically and tightly bind the toxic oligomers over monomeric and fibrillar forms of Aβ, leading to inhibition of aggregation in vitro and neurotoxicity in neuroblastoma cells. Based on this specific binding, a soluble oligomer-binding assay (SOBA) was developed as an indirect probe of α-sheet content. Combined SOBA and toxicity experiments demonstrate a strong correlation between α-sheet content and toxicity. The designed α-sheet peptides are also active in vivo where they inhibit Aβ-induced paralysis in a transgenic Aβ *Caenorhabditis elegans* model and specifically target and clear soluble, toxic oligomers in a transgenic APPsw mouse model. The α-sheet hypothesis has profound implications for further understanding the mechanism behind AD pathogenesis.

α-sheet | toxic soluble oligomers | Alzheimer's disease | soluble oligomer binding assay | amyloid beta

A mechanistic explanation for the role of the β-amyloid peptide (Aβ) in Alzheimer's disease (AD) has eluded scientists for over 50 y, with advancing technologies and discoveries seemingly further confounding the understanding of the disease—a modern iteration of Zeno's Paradox. Monomeric Aβ has been associated with a variety of biological functions, including memory, learning, and neuroprotection (1–6). The modified amyloid cascade hypothesis, the prevailing theory of pathogenesis, adds additional complexity to the study of the disease by implicating a dynamic and heterogeneous distribution of soluble Aβ oligomers as the primary toxic agents and asserting that the resultant amyloid fibrils are relatively benign (7–17). Furthermore, the toxic soluble oligomers are correlated with disease progression while amyloid burden is not (12, 13, 18–20). The ability of the A11 oligomer-specific antibody to recognize and block toxicity in a variety of amyloid systems illustrates the importance of these oligomers (21). The cross-reactivity of the A11 antibody suggests that soluble oligomers share a conformational, rather than sequence-based, epitope that promotes structural uniformity upon deposition, as determined for the fibrillar state by a variety of spectroscopic methods (22–25). A similar conclusion was reached based on atomistic molecular dynamics simulations in which we discovered a secondary structure—α-sheet—that is adopted by unrelated proteins under amyloidogenic conditions (26). We proposed that it is linked to aggregation and toxicity of the soluble oligomers and is the common structure targeted by the A11 antibody (26–28). Outwardly, α-sheets resemble β-sheets except that the carbonyl oxygens are aligned on one face of a strand and the NH groups on the other instead of alternating, which gives rise to different physical properties (28, 29) (*SI Appendix*, Fig. S1). Here, we investigate the implications of the α-sheet hypothesis using a variety of experimental techniques. Aggregation of Aβ (1–42)—hereafter referred to as Aβ—was monitored over time by several biophysical methods. Aβ has a high propensity to form soluble oligomers containing α-sheet structure, and the extent of α-sheet is correlated with toxicity. Novel synthetic α-sheet peptides designed to bind to the predicted α-sheet structure from simulations specifically bind toxic Aβ oligomers, inhibit aggregation in vitro, and protect against toxicity in cell-based assays and in two animal models: *Caenorhabditis elegans* and transgenic APPsw mice.

Aβ Forms Toxic Oligomers During the Lag Phase of Aggregation

To assess the oligomeric behavior of Aβ, a standard thioflavin T (ThT) fluorescence binding assay was employed to monitor its aggregation at pH 7.6 in PBS. ThT binding is generally assumed to reflect formation of β-sheet fibrils. Sigmoidal kinetics were observed, indicative of a nucleation polymerization pathway (30) (Fig. 1*A*). There was a pronounced lag phase before a sharp increase in ThT binding and fibril formation with modulations of the onset of aggregation dependent on concentration as well

Significance

There have been over 400 clinical trials for Alzheimer's disease, all targeting the monomeric and/or fibrillar forms of the Aβ peptide to curb amyloid burden; however, it is the toxic soluble oligomers that are correlated with disease progression, not mature amyloid. Here we provide evidence that Aβ soluble oligomers adopt a nonstandard secondary structure: α-sheet. This structure forms early in aggregation and is strongly correlated with toxicity. Furthermore, designed de novo α-sheet peptides target the toxic oligomers, inhibiting aggregation and toxicity in vitro in cell-based assays and in vivo in two different animal models. This work challenges the prevailing dogma and sheds light on potential new approaches to the problem.

Author contributions: D.S., J.Z., G.V., C.D.L., M.M., and V.D. designed research; D.S., C.-C.H., T.M.B., N.P., M.C.C., J.C., C.P.T., L.W., and D.P. performed research; D.S., C.-C.H., T.M.B., N.P., M.C.C., C.P.T., L.W., D.P., C.D.L., M.M., and V.D. analyzed data; and D.S., D.P., G.V., C.D.L., M.M., and V.D. wrote the paper.

The authors declare no conflict of interest.

This article is a PNAS Direct Submission.

Published under the PNAS license.

Data deposition: The NMR data reported in this paper have been deposited in the BioMagResBank, www.bmrb.wisc.edu (accession no. 27873).

[1]To whom correspondence should be addressed. Email: daggett@uw.edu.

This article contains supporting information online at www.pnas.org/lookup/suppl/doi:10.1073/pnas.1820585116/-/DCSupplemental.

Published online April 19, 2019.

Downloaded at Palestinian Territory, occupied on December 7, 2021

www.manaraa.com

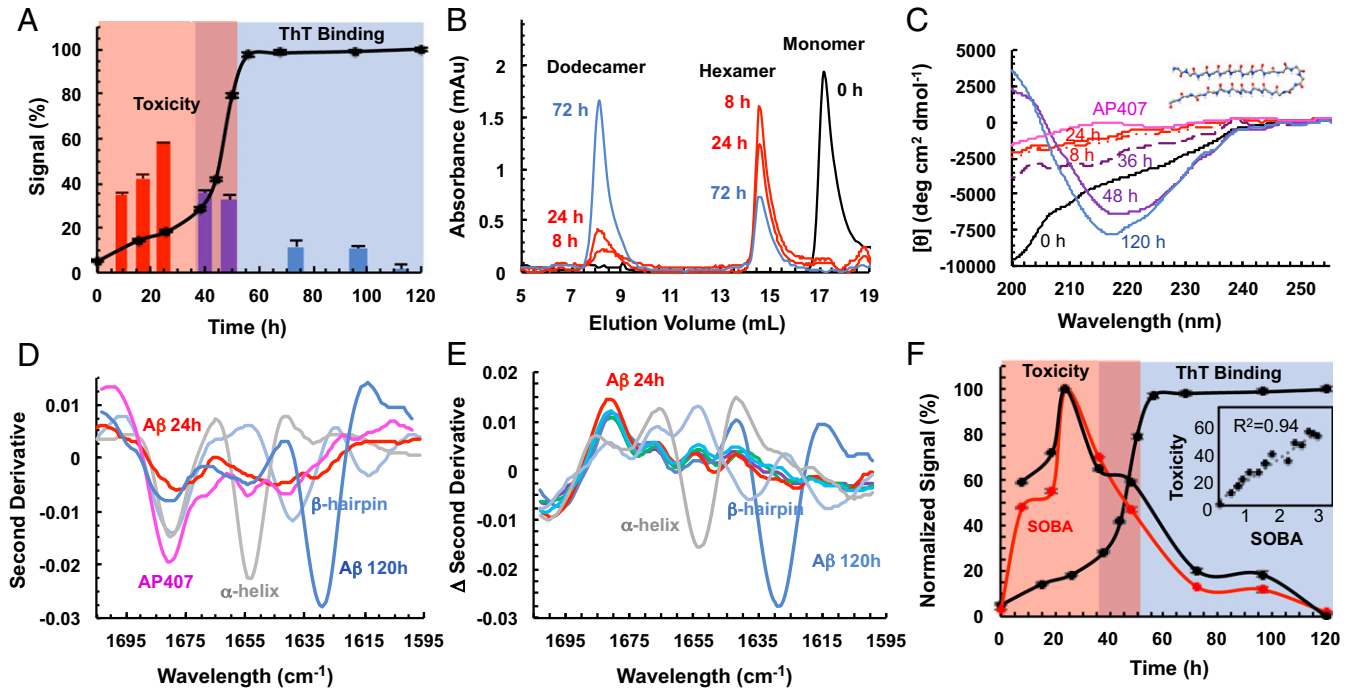

Fig. 1. Determination of Aβ aggregation kinetics, toxicity, and structure. (*A*) ThT binding assay with 75 μM Aβ at 25 °C in PBS buffer with 24 μM ThT. MTT cell toxicity assay for preincubated 75-μM Aβ species at 25 °C in PBS, diluted to 30 μM in media before applying to cells. Cell toxicity peaks in the lag phase at 24 h and recovers as β-sheet content exponentially increases. (*B*) SEC traces of Aβ aggregate development over time from monomer to hexamer to dodecamer and then larger-molecular-weight species. (*C*) CD spectra of 75-μM Aβ monomer in NaOH (black), oligomeric Aβ in PBS at 8 h of incubation (dash-dot-dot red), 24 h of incubation (solid red), 36 h of incubation (dashed purple), 48 h of incubation (purple), 120 h of incubation (blue), and 45-μM designed α-sheet peptide AP407 (magenta) in PBS. Structure #7 of the NMR-derived structural ensemble of AP407 is displayed next to its CD spectrum (see *SI Appendix*, Fig. S4 for the full NMR ensemble). The 8- and 24-h Aβ samples are relatively nondescript, similar to the "null" signal shown for AP407, suggestive of α-sheet structure in oligomeric Aβ. (*D*) MMS spectra for control peptides and 75-μM oligomeric Aβ (24 h in red and 120 h in dark blue). α-Sheet spectrum (AP407, magenta) is distinct from α-helix (PSMα1 peptide in gray) and β-hairpin (P411, light blue). Toxic oligomeric Aβ (24 h) tracks very closely with the α-sheet curve. (*E*) The difference in second derivative spectra of MMS was obtained by subtracting the AP407 α-sheet signal from all other samples including other α-sheet designs. The 24-h Aβ oligomer tracks with the α-sheet designs and not α-helical nor β-sheet structure. In contrast, the 120-h β-sheet fibrils are similar to the β-hairpin but shifted to lower wavenumbers, as is commonly seen for amyloid fibrils (44). (*F*) SOBA binding intensities (plotted with MTT toxicity and ThT binding) from *A*. Aβ samples were applied at a concentration of 250 nM to optimize the ratio of the specific/nonspecific binding signals (*SI Appendix*, Fig. S5). Binding is highest at 24 h, when β-sheet content is low. As β-sheet content increases exponentially, SOBA binding decreases. Both α-sheet content and toxicity peak in the lag phase of aggregation and are strongly correlated (*Inset*). Points with closed circles were all performed with 75-μM Aβ, whereas points with open circles were performed with 25 μM Aβ; despite differences in concentration, the correlation remains. All data points presented are based on $n \geq 3$.

as the fluorescence measurement frequency due to robotic action of the plate reader (*SI Appendix*, Fig. S2*A*). To align the various experiments, we used the kinetics for the "undisturbed" method (Fig. 1*A*, 36 h lag; *SI Appendix*, Fig. S2*A*) as the frame of reference for most experiments, from which aliquots were removed at various times during aggregation to investigate the structure and toxicity of the samples. As we are interested in characterizing species populated during aggregation using different methods, the kinetic stability of the aliquots was assessed by storing preincubated Aβ on ice at 4 °C for up to 300 h and taking periodic ThT measurements. Storing samples on ice stalled aggregation, which recommenced when the samples were brought back to 25 °C (*SI Appendix*, Fig. S2 *B* and *C*).

After establishing conditions for reproducible kinetics and stability of time-dependent samples for further analysis, we evaluated the effect of Aβ on cell viability, which was indirectly measured by mitochondrial function as a surrogate for toxicity in SH-SY5Y neuroblastoma cells. Samples matched with those of the ThT assay showed increasing toxicity during the lag phase, which peaked at 24 h (Fig. 1*A*). The toxicity trend indicated that Aβ was most toxic during the lag phase and did not appear to involve β-sheet structure, as reflected in the lack of ThT binding. In contrast, the β-sheet–rich fibrils were relatively nontoxic. Similar results were obtained by Luo et al. (31) for Aβ (1–40). In addition, Giuffrida et al. (1) established that high-molecular-weight aggregates contain predominantly β-structure, whereas the low-molecular-weight aggregates are much more heterogeneous and dynamic in both size and structure. Consequently, we characterized the size and structure distributions of the Aβ aggregates over time, particularly those associated with toxicity in the lag phase.

To characterize the size distribution of the Aβ aggregates over time, we employed size exclusion chromatography (SEC) (Fig. 1*B*; see standard curve in *SI Appendix*, Fig. S3). Early in aggregation, the Aβ monomers converted to small oligomers, with hexamers being the dominant species; however, it should be noted that these SEC measurements are not precise enough to rule out pentamers, for example. Over time, the hexamer peak decreased and a broad, higher-molecular-weight peak appeared, corresponding to dodecamers and larger species (further referred to as dodecamer). Primarily higher order species were obtained during the plateau phase of the ThT curve. Interestingly, we did not observe a multitude of oligomers but instead only two main populations: hexamers and dodecamers in equilibrium, shifting over time both during the lag phase and beyond (Fig. 1*B*).

Oligomers derived from human brains have molecular weight distributions corresponding to a mix of dimers to dodecamers, and the dodecamer in particular has been linked to disease (20, 32–34). For example, dodecamers derived from transgenic (Tg) APP-overexpressing mice impair memory when injected into brains of young rats (32). Dissociation of dodecamers into trimers and tetramers leads to cognitive recovery in mouse models (35), while hexamers are in dynamic equilibrium with the dodecamers [also referred to as Aβ*56 in the literature based on molecular weight (20)]. We did not observe the smaller oligomers that have been

Downloaded at Palestinian Territory, occupied on December 7, 2021
www.manaraa.com

observed by SDS/PAGE and SDS purification from brain, such as dimers, trimers, and tetramers, which some have suggested may be the result of the dissolution of larger aggregates (36, 37). Thus, the lack of small oligomers and the existence of the dodecamers obtained here at neutral pH in PBS suggest that we are likely probing physiologically relevant oligomeric species.

Toxic Oligomers Contain α-Sheet Structure, Not β-Sheet Structure

The secondary structure of Aβ was then evaluated as a function of time by circular dichroism (CD) (Fig. 1*C*). Consistent with the ThT profile, aggregation initiated from an unstructured random coil conformation (0 h) and proceeded to β-sheet structure in the course of aggregation (48 h and beyond). Interestingly, the curve lifted and flattened in the lag phase before β-sheet formation (shown for 8–36 h). Thus, the hexamer and dodecamer oligomers populated during the lag phase do not contain measurable conventional secondary structure, while the higher-molecular-weight late species (48 h and beyond) contain β-structure consistent with the inference from the ThT-binding assay. The featureless CD spectra of the intermediate oligomers (in both size and time) are similar to what we proposed and confirmed experimentally for α-sheet structure (29, 38–40). Designed α-sheet peptides (denoted as AP#, for alternating peptide) produce a "null signal" due to their unique structural characteristics that lead to cancellation of the CD signal, as shown in Fig. 1*C* for the α-sheet design AP407, which is distinct from random coil, α-helical, and β-sheet CD spectra (29, 38–40). Contrary to our results, many assume that Aβ soluble oligomers adopt β-sheet structure in the lag phase, but a number of other studies report CD spectra very similar to the α-sheet spectra provided here (17, 31, 41, 42). While similar spectra were obtained, they were not recognized to be α-sheet due to its novelty, as model compounds are critical to the assignment of spectra. Here we used our synthetic α-sheet designs, such as AP407, for that purpose, but to do so, further characterization of the structure was necessary.

To obtain more detailed structural information for our α-sheet designs, 2D NMR experiments of AP407 were performed, which resulted in 455 distinct nuclear Overhauser effect interactions (NOEs) between protons for this 23-residue peptide (Dataset S1), allowing for the calculation and testing of structural models of AP407 (*SI Appendix*, Fig. S4*A*). The chemical shifts from NMR and the NMR-derived structural ensemble are in excellent agreement (*SI Appendix*, Fig. S4*B*). The secondary chemical shifts, which are often used to determine regions of secondary structure, are consistent with α-helical structure while the coupling constants reflecting the Φ dihedral angles are not (*SI Appendix*, Fig. S4*C*). Instead, the coupling constants are indicative of β-sheet or extended structure. Thus, the NMR results point to both α-helix and extended sheet structure, as we would expect for an α-sheet comprised of local helical (Φ,Ψ) values of alternating chirality (*SI Appendix*, Fig. S1) forming a hairpin sheet structure. The NOEs provide further support for this conclusion. Sequential H_N-H_N NOEs expected for α-sheet structure were observed, while the standard main-chain NOE patterns expected for α-helical and β-sheet structures were not present (*SI Appendix*, Fig. S4 *D* and *E*), which is consistent with the flat CD spectrum for AP407 (Fig. 1*C*, with one of the NMR structures provided in the *Inset*). In an earlier study, we obtained NOEs for two other α-sheet designs, but not a sufficient number to calculate a structure (38). Here, however, we obtained a greater number of NOEs —including side-chain NOEs—by using a more constrained design with a disulfide bond linking the α-strands. One hundred percent of the 455 NOEs are satisfied by the ensemble presented in *SI Appendix*, Fig. S4. As is generally the case with small peptides, however, AP407 retains conformational flexibility, as is particularly evident in the turn region due to alternative side-chain packing (*SI Appendix*, Fig. S4*A*).

Microfluidic modulation spectroscopy (MMS) was used to further characterize the structural characteristics of Aβ during aggregation. MMS measures peptide absorption spectra by optically scanning across the amide I band, which reflects a combination of patterns of hydrogen bonding, dipole–dipole interactions, and the geometric orientations throughout the peptide. As this is a new technique and α-sheet is a nonstandard structure, we used synthetic designed α-sheet hairpins as model compounds to help interpret the spectra, along with controls for other conventional secondary structures: designed α-sheet hairpins (AP5, AP90, AP407, and AP421), β-sheet (P411), and α-helical (PSMα1) peptides (sequences and color mapping provided in *SI Appendix*, Table S2). Each class of peptide produced distinctive spectral features, as shown in the second derivative plots of the amide I region (Fig. 1*D*). This is further illustrated by subtracting the AP407 α-sheet peptide spectrum from the other samples, highlighting the similarities between the different α-sheet peptides with the largest difference at 1,680 nm, which we surmise is due to the improved dipole alignment from stabilization of the α-sheet structure in the hairpin due to the disulfide cross-link (Fig. 1*E*). Moreover, this band was predicted to be dominant for nonsolvated α-sheet structure (43) and confirmed experimentally by conventional Fourier-transform infrared spectroscopy (FTIR) of dry films (29, 38, 39).

After establishing the spectral features of the model compounds, we analyzed the most toxic Aβ sample (24 h) and found its spectrum to be consistent with α-sheet and distinct from β-sheet and α-helix (Fig. 1 *D* and *E*). In fact, the Aβ oligomer spectrum nicely overlays the other α-sheet spectra. With increasing aggregation time, the Aβ spectrum shifted and was most similar to our β-sheet control (P411) rather than any of our α-sheet designs (120 h, Fig. 1 *D* and *E*), but note the shift in the 120-h Aβ sample relative to the monomeric β-hairpin P411. Such shifts are routinely seen between conventional β-structure and fibrils by FTIR (44). Consistent with the ThT and CD results, the α-sheet structure preceded β-sheet formation. In addition, it was recently found that fibrils of a fragment of a variant of the amyloidogenic protein transthyretin contain spectroscopic signals of both α-sheet and β-sheet structures by FTIR, providing further support for the presence of α-sheet in amyloid systems and the possibility of coexistence of an α- and β-sheet (27, 45).

De Novo α-Sheet Peptides Specifically Bind Toxic Oligomers

The CD, FTIR, and NMR results all support the presence of α-sheet secondary structure in our designed peptides, and the toxic oligomeric Aβ samples are essentially indistinguishable from the peptides. As another probe of α-sheet content during aggregation, we developed the soluble oligomer-binding assay (SOBA), which is an ELISA-like assay that utilizes an α-sheet peptide (AP193) instead of an antibody as the capture agent. Under the conditions used here, SOBA detects α-sheet content in toxic Aβ solutions at concentrations below 2.5 nM, corresponding to ∼1.1 ng (*SI Appendix*, Fig. S5). In effect, SOBA is an indirect reporter of α-sheet structure owing to the binding via complementary α-sheet structure in the designed peptide and the amyloid species. Consistent with the ThT, CD, and MMS experiments, SOBA-detected α-sheet structure was highest in the lag phase and preceded the formation of β-structure (Fig. 1*F*). The progression of α-sheet corresponded with cell toxicity and revealed that both peaked at 24 h and decreased drastically as β-sheet content increased exponentially. Importantly, there was a strong correlation between α-sheet formation by SOBA and cell toxicity ($R^2 = 0.94$, Fig. 1*F*, *Inset*), supporting our hypothesis that oligomeric α-sheet structure is associated with toxicity.

SEC was then used to assess the affinity of α-sheet designs for soluble, toxic Aβ oligomers of different sizes. First, excess AP407 was added to monomeric Aβ (4:1 by concentration), and there was no effect on the elution curve (Fig. 2*A*). However, addition of AP407 to Aβ preincubated for 24 h at 25 °C resulted in a shift in both the hexamer and dodecamer peaks toward higher molecular weights consistent with specific binding of the peptide to these assemblies (Fig. 2*A*). Additionally, biolayer interferometry was employed to quantify the binding kinetics of individual SEC fractions to the AP5 α-sheet peptide design. The hexamer peak from an 8-h incubation and the dodecamer peak from a 24-h

Downloaded at Palestinian Territory, occupied on December 7, 2021

www.manaraa.com

incubation had nanomolar binding affinities (0.48 and 8.1 nM, respectively) (*SI Appendix*, Table S3).

α-Sheet Peptides Inhibit Aβ Aggregation and Cytotoxicity

Having shown that designed α-sheet peptides bind to toxic oligomeric aggregates of Aβ specifically and tightly, we assessed their ability to inhibit aggregation using the ThT assay. Overall, incubation of Aβ with α-sheet designs in excess (4:1) reduced aggregation by up to 96% while the random coil (P1) and β-sheet (P411) controls had no significant effect (Fig. 2*B*). The α-sheet peptides inhibited aggregation by binding the complementary structure in the toxic soluble oligomers in the lag phase (Fig. 2*A*), which are on-pathway to aggregation (*SI Appendix*, Fig. S2 *B* and *C*). We then tested whether inhibition also led to neutralization of toxicity using a preincubated 24-h Aβ sample with AP5 or AP421 (Fig. 2*C*). Cell viability was recovered upon addition of the α-sheet designs, confirming that the inhibitory effect targeted the toxic oligomers. Notably, the peptides alone (hashed bars in Fig. 2*C*) were not toxic although they too contain α-sheet structure, but by design they remain monomeric to avoid toxicity.

To investigate the hypothesis that the A11 antibody recognizes toxic oligomers with different sequences through α-sheet structure, we performed dot-blot experiments with the A11 antibody and our α-sheet peptides (21). As expected, A11 bound toxic Aβ oligomers (red bars, preincubated 24 h) while binding to fibril samples was negligible (Fig. 2*D*). Interestingly, A11 bound designed α-sheet peptides with high intensity comparable to Aβ oligomers (67 and 80% of A11 positive control for AP407 and AP5, respectively, compared with 63% for Aβ), while values for the random coil (P1) and β-sheet (P411) controls were negligible. Recognition of the α-sheet motif by an oligomer-specific antibody supports the assertion that this structure is present in toxic Aβ oligomers. Furthermore, incubation of Aβ with α-sheet peptides (1:1 by mass) decreased A11 binding intensity, even if each bound with roughly equivalent intensity alone (Fig. 2*D*, red bars). The reduction in intensity is shown relative to the A11 primary signal, but as both Aβ and the α-sheet peptides bind the A11 antibody, the effect is even greater when normalized by the sum of the observed Aβ and α-sheet peptide signals, leading to a drop of 35 and 27% for AP407 and AP5, respectively. This substantial drop in A11 binding suggests that the binding of the Aβ oligomers to the AP peptides alters their conformations, thereby changing the A11 epitopes, or that the antibody-binding sites are masked in the Aβ-AP407 complex. The CD spectra for the oligomer with and without AP407 are indistinguishable (*SI Appendix*, Fig. S6), supporting the latter interpretation that the epitopes are masked when AP407 binds Aβ. Thus, the A11 antibody and α-sheet peptides appear to share a common binding epitope on toxic Aβ oligomers. In contrast, incubation of Aβ with random coil and β-sheet peptides had no significant effect.

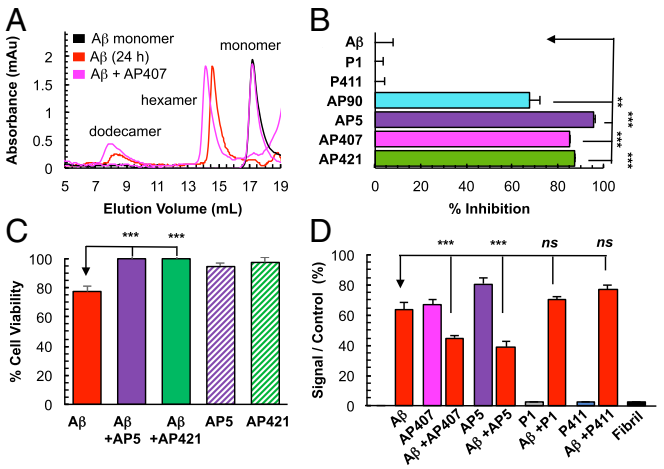

Fig. 2. α-Sheet specificity for oligomeric Aβ. (*A*) SEC traces of 75-μM monomeric Aβ with and without α-sheet peptide added. The traces are essentially identical, indicating that AP407 does not bind to monomeric Aβ. The 75-μM oligomeric (24 h) Aβ with and without AP407. The peak shift of ∼0.4 mL to higher molecular weight upon addition of α-sheet peptide indicates binding to the oligomeric aggregates of Aβ. (*B*) Effect of α-sheet, β-sheet, and random coil peptides on Aβ aggregation obtained via ThT fluorescence. The 25 μM Aβ was coincubated with excess (4:1) peptide and the fluorescence was measured at 144 h. α-Sheet peptides of different sequence inhibited aggregation whereas β-sheet (P411) and random coil (P1) controls had no significant effect. (*C*) Neutralization of toxicity by α-sheet peptides. The 25-μM Aβ was preincubated for 24 h (see *SI Appendix*, Fig. S2*A* for ThT kinetics) and applied to cells at a concentration of 10 μM. Addition of α-sheet peptides resulted in full recovery of cell viability. The AP peptides were not toxic to the cells (hashed bars). (*D*) Dot blot with the A11 oligomer-specific antibody used as the primary. A11 specifically recognizes the Aβ oligomer (20-h incubation at 110 μM in H_2O) and α-sheet peptides but not the random coil and β-sheet peptide controls or fibrils. Peptides were then coincubated with Aβ for 20 h and blotted on the membrane to investigate competition between the α-sheet peptides and A11 for the binding domain on oligomeric Aβ. Coincubation reduced the overall signal with α-sheet peptides added but not the random coil and β-sheet peptides. Signals were integrated using ImageJ software after background subtraction. Following integration, signals were normalized to fraction A11 signal: i.e., < peptide signal >/< A11 signal >, where the brackets indicate average values. All data presented are based on $n \geq 3$. Statistical significance: $^{**}P < 0.01$, and $^{***}P < 0.001$.

α-Sheet Designs Decrease Toxic Oligomers in AD Mouse Model

Next, we investigated the effect of administering an α-sheet design (AP5) to transgenic (Tg) APPsw mice expressing human Aβ (1–42) both ex vivo (46) and in vivo (47). The ex vivo system involved testing the effect of AP5 on 250-μm thick brain sections from 91-wk-old Tg APPsw mice. Coronal brain sections were excised and treated with either PBS (control vehicle to dissolve AP5) or AP5 and cultured for 24 h before quantification and analysis. AP5 had no significant effect on average protein concentrations or, as a more specific probe, lactate dehydrogenase released after 24 h in soluble fractions of brain slice homogenates (*SI Appendix*, Fig. S7 *A* and *B*), indicating that AP5 did not induce toxicity in the organotypic brain slice cultures and that the brain tissue was still viable. The A11 antibody was used to assess toxic oligomer levels in the detergent soluble fraction of the brain slice homogenates with and without AP5 treatment. AP5 had no effect on detergent insoluble levels of Aβ (amyloid fibrils and plaques) (*SI Appendix*, Fig. S7 *C* and *D*), whereas the A11-detectable oligomers were reduced in a dose-dependent manner with a maximum drop of 79% (Fig. 3*A*). To further evaluate the effects of AP5 on Aβ oligomers, the detergent-solubilized fractions of brain slice homogenates were analyzed by Western blots using the 6E10 Aβ antibody under nondenaturing conditions, which showed a maximum drop of 82%, confirming the A11 results (*SI Appendix*, Fig. S7*E*). In contrast, the total Aβ dropped by 44% at the highest dose of AP5, with the largest decrease in the Aβ42 population (Fig. 3*B*). These findings show that the preferential binding of the toxic oligomers presented above in vitro and in the cell-based assay were also operative ex vivo in the organotypic brain slices from Tg APPsw mice.

Following the encouraging results in brain sections, AP5 was administered via intracranial injection to the right hemisphere (hippocampus and cortex) of 103-wk-old Tg APPsw mice. A11-detectable oligomers were assessed 24 h later and were found to drop by up to 40% (compared with the left hemisphere control of the same animal, Fig. 3*C*). It is noteworthy that these animals were in the late stages of cerebral amyloidosis, where anti-amyloid interventions typically have limited effects, and, as above, A11 binding to AP5 may be contributing to the signal, masking some of the effect. Recently, Luo et al. (48) reported a self-destructive nanosweeper that captures and clears Aβ by activating autophagy. However, this nanosweeper recognizes Aβ by a sequence-complementarity motif and thus indiscriminately captures and clears monomers as well as oligomers. In contrast, the α-sheet

Downloaded at Palestinian Territory, occupied on December 7, 2021
www.manaraa.com

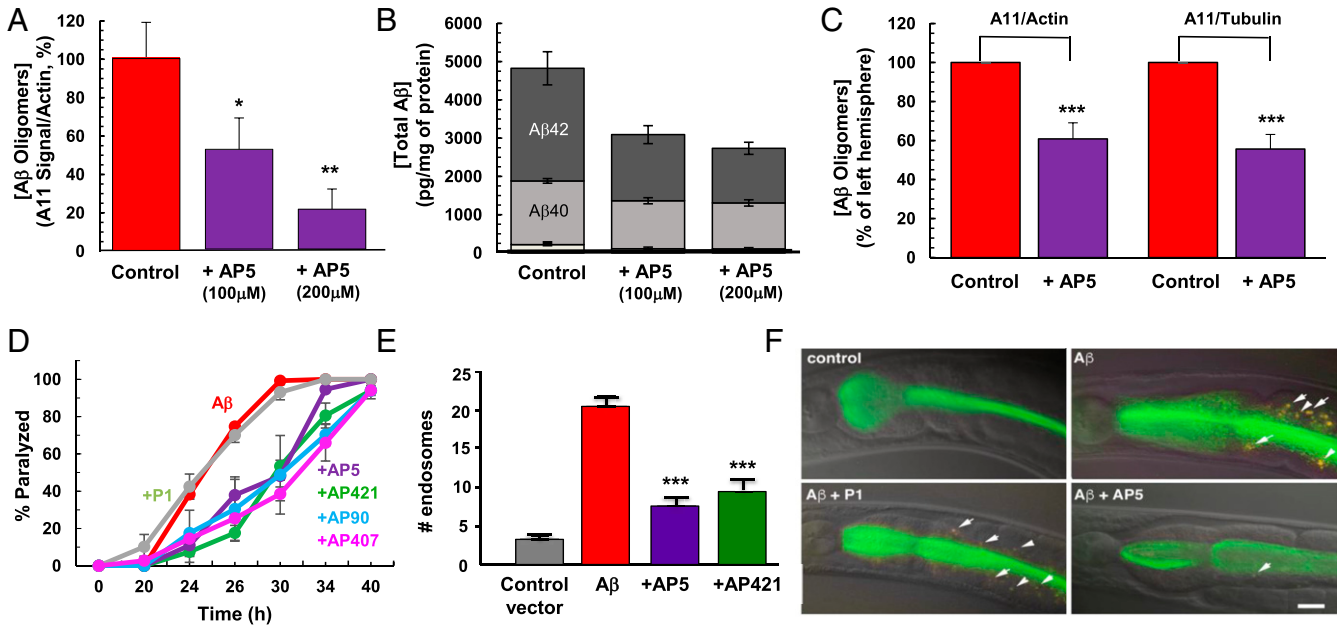

Fig. 3. The effect of α-sheet peptides in transgenic mice and *C. elegans* expressing human Aβ. (*A*) A11 detectable oligomers were reduced in the presence of AP5 in ex vivo TgAPPsw brain slices. The oligomers decreased by 48 and 79% after addition of 100 and 200 μM AP5, respectively, in the detergent soluble fractions. Oligomer content is expressed relative to the reference protein actin. (*B*) Detergent soluble Aβ38, Aβ40, and Aβ42 quantified using an Aβ ELISA test. Aβ38 is the minor, unlabeled component at the bottom of each bar. (*C*) A11-detectable oligomers decreased by 40% in the right hemisphere injected with AP5 compared with the control left hemisphere. Values were determined using two different reference proteins, actin and tubulin. These results, both ex vivo and in vivo, indicate that AP5 specifically targeted the soluble, toxic oligomers. (*D*) Quantification of the effect of α-sheet peptides and controls on Aβ-induced paralysis in transgenic *C. elegans* expressing human Aβ. Random coil (P1) peptide tracked closely with Aβ-only control while the α-sheet peptides were able to maintain nonparalyzed populations for much longer (statistically significant by Kaplan–Meier, log rank, and Mantel–Cox tests). (*E*) Quantification of Aβ-induced membrane disruption, tracked via extent of endosome formation, with and without α-sheet peptides in *C. elegans* that ingest human Aβ-secreting *E. coli* or control wild-type *E. coli* with α-sheet peptides in the culture media. Addition of α-sheet peptide closely resembled empty vector control, indicating efficacy of AP5 and AP90 in treating this transgenic GFP reporter strain GK280 of *C. elegans*. (*F*) Representative images of the anterior intestine of GFP reporter strain GK280 [***dkIs166***(P*opt-2*::GFP::*pgp-1*)] fed engineered cultures of *E. coli* expressing human Aβ (1–42) pretreated with a control or α-sheet peptide. (*Top Left*) Reporter strain fed *E. coli* expressing control empty vector. (*Top Right*) Reporter strain fed *E. coli* secreting Aβ. (*Bottom Left*) Aβ pretreated with control, random coil peptide P1. (*Bottom Right*) Aβ pretreated with AP5. Strains were co-fed with Texas Red-dextran to monitor active feeding, resulting in endosomes labeled with both GFP and Texas Red. Images are digital overlays of epifluorescence and differential interference contrast images. (Scale bar, 10 microns.) Data presented in *A–C* are based on $n \geq 10$ and in *D* and *E* on $n \geq 30$. Statistical significance is indicated as $^{*}P < 0.05$, $^{**}P < 0.01$, and $^{***}P < 0.001$.

peptide AP5 was associated with clearance of toxic Aβ in a dose-dependent manner (Fig. 3*A* and *SI Appendix*, Fig. S7*E*), suggesting a mechanism based on structure rather than sequence recognition, thereby selectively removing pathogenic forms of Aβ while leaving monomers and nontoxic fibrils intact.

α-Sheet Peptides Inhibit Aβ-Induced Paralysis in AD *C. elegans* Model

Given the difficulty of long-term administration of compounds in transgenic mouse AD models, we sought an alternative model system to test the ability of α-sheet peptides to block Aβ toxicity in vivo. We chose a transgenic *C. elegans* model that has been used extensively to assay the ability of exogenous compounds to reduce Aβ toxicity (49). Upon temperature upshift, the transgenic *C. elegans* strain CL4176 up-regulates Aβ expression in body-wall muscle, leading to a reproducible paralysis phenotype (49). While in the past it has been difficult to treat *C. elegans* with large molecules such as peptides or proteins, Perni et al. (50) showed that treating *C. elegans* with a novel cationic lipid vesicle transfection reagent allows ingested proteins to spread throughout the body. Using a FITC-labeled α-sheet peptide, we confirmed that coexposure with the transfection reagent allowed whole-body exposure to the peptide (*SI Appendix*, Fig. S8). We then tested whether exposure to a set of α-sheet peptides would delay the onset of paralysis induced by Aβ up-regulation in strain CL4176. All α-sheet peptides tested (AP5, AP90, AP407, and AP421) significantly delayed Aβ-induced paralysis, while the control random coil peptide P1 had no effect (Fig. 3*D*). These worms rarely form amyloid plaques, such that the paralysis is not associated with plaque burden (51), and instead, inducible Aβ expression leads to the formation of toxic soluble oligomers, which is consistent with the observed mechanism of inhibition by α-sheet compounds.

The transgenic *C. elegans* experiments described above cannot determine whether the protective effects of the α-sheet peptides result from their direct interaction with Aβ, as predicted by our proposed mechanism of action, or from an unknown interaction downstream in the toxic process. We therefore employed another *C. elegans* model in which transgenic GFP reporter worms were fed *Escherichia coli* engineered to secrete human Aβ (1–42) (52). *C. elegans* ingestion of Aβ-expressing *E. coli* leads to intestinal membrane damage, which can be measured by quantifying induced endosomes labeled with a GFP fusion protein that normally localizes to the intestinal lumen (52). This model allowed us to pre-expose Aβ to the peptides (by treating the *E. coli* cultures rather than the worms) before assaying Aβ toxicity. As shown in Fig. 3 *E* and *F*, treating the Aβ-expressing *E. coli* culture with α-sheet peptides significantly inhibited the induction of intestinal endosomes that normally occurs when these cultures are fed to the *C. elegans* reporter strain. We interpret this result to indicate that the α-sheet peptides are interacting with Aβ secreted by the *E. coli* strain and neutralizing the toxic oligomers.

Conclusions

AD is associated with a heterogeneous distribution of toxic oligomers, making it difficult to discern mechanisms of toxicity.

Downloaded at Palestinian Territory, occupied on December 7, 2021
www.manaraa.com

Here, we isolated and characterized a unique secondary structure motif—α-sheet—in specific populations of Aβ oligomers associated with neurotoxicity. We showed that the α-sheet structure is recognized by the A11 amyloid-oligomer–specific antibody, that α-sheet peptides inhibited Aβ aggregation and blocked toxicity, and that α-sheet peptides bound specifically to oligomeric preparations of Aβ. Furthermore, α-sheet peptides specifically recognized and neutralized the toxic, soluble oligomers of Aβ in two very different animal models of AD. These findings open the possibility of novel therapeutic and diagnostic agents for AD and other amyloid diseases.

Methods

Aβ (1–42) was obtained from the ERI Amyloid Laboratory LLC. The α-sheet and other control peptides were produced manually by solid-phase peptide synthesis. The aggregation conditions were optimized to provide reproducible kinetics under undisturbed conditions for investigation of samples by different techniques as a function of time, including structural studies and interactions between Aβ and α-sheet peptides by a variety of biophysical approaches, as well as in immortalized cells and two animal models. A detailed description of the methods is provided in *SI Appendix*.

ACKNOWLEDGMENTS. V.D. thanks Drs. James Bryers, Xiaohu Gao, Cecilia Giachelli, Gene Hopping, Jackson Kellock, and Suzie Pun. V.D. was supported by NIH Award GMS 95808, University of Washington Office of Research, University of Washington CoMotion, and University of Washington Bioengineering Department. This work was also supported by the University of Washington Mary Gates Fellowship Program (C.-C.H. and N.P.) and a Washington Research Fellowship (to T.M.B.). C.D.L. was supported by NIH Award R21AG049693, and C.P.T. was supported by an American Microscopy Society Fellowship. G.V. acknowledges support from NIH–National Institute of General Medical Sciences and the NSF. M.M. acknowledges support from the Roskamp Foundation.

1. Giuffrida ML, et al. (2010) The monomer state of β-amyloid: Where the Alzheimer's disease protein meets physiology. *Rev Neurosci* 21:83–93.
2. Whitson JS, Selkoe DJ, Cotman CW (1989) Amyloid β protein enhances the survival of hippocampal neurons *in vitro*. *Science* 243:1488–1490.
3. Morley JE, et al. (2010) A physiological role for amyloid-β protein: Enhancement of learning and memory. *J Alzheimers Dis* 19:441–449.
4. Bishop GM, Robinson SR (2004) Physiological roles of amyloid-β and implications for its removal in Alzheimer's disease. *Drugs Aging* 21:621–630.
5. Hiltunen M, van Groen T, Jolkkonen J (2009) Functional roles of amyloid-beta protein precursor and amyloid-beta peptides: Evidence from experimental studies. *J Alzheimers Dis* 18:401–412.
6. Koudinov AR, Berezov TT (2004) Alzheimer's amyloid-β (A β) is an essential synaptic protein, not neurotoxic junk. *Acta Neurobiol Exp (Warsz)* 64:71–79.
7. Selkoe DJ (2001) Alzheimer's disease: Genes, proteins, and therapy. *Physiol Rev* 81: 741–766.
8. Mullan M, et al. (1992) A pathogenic mutation for probable Alzheimer's disease in the APP gene at the N-terminus of beta-amyloid. *Nat Genet* 1:345–347.
9. Masters CL, et al. (1985) Amyloid plaque core protein in Alzheimer disease and Down syndrome. *Proc Natl Acad Sci USA* 82:4245–4249.
10. Glenner GG, Wong CW, Quaranta V, Eanes ED (1984) The amyloid deposits in Alzheimer's disease: Their nature and pathogenesis. *Appl Pathol* 2:357–369.
11. McLean CA, et al. (1999) Soluble pool of Abeta amyloid as a determinant of severity of neurodegeneration in Alzheimer's disease. *Ann Neurol* 46:860–866.
12. Haass C, Selkoe DJ (2007) Soluble protein oligomers in neurodegeneration: Lessons from the Alzheimer's amyloid β-peptide. *Nat Rev Mol Cell Biol* 8:101–112.
13. Lambert MP, et al. (2001) Vaccination with soluble Abeta oligomers generates toxicity-neutralizing antibodies. *J Neurochem* 79:595–605.
14. Wang J, Dickson DW, Trojanowski JQ, Lee VM (1999) The levels of soluble versus insoluble brain Abeta distinguish Alzheimer's disease from normal and pathologic aging. *Exp Neurol* 158:328–337.
15. Yang T, Li S, Xu H, Walsh DM, Selkoe DJ (2017) Large soluble oligomers of amyloid β-protein from Alzheimer brain are far less neuroactive than the smaller oligomers to which they dissociate. *J Neurosci* 37:152–163.
16. Lambert MP, et al. (1998) Diffusible, nonfibrillar ligands derived from Abeta1-42 are potent central nervous system neurotoxins. *Proc Natl Acad Sci USA* 95:6448–6453.
17. Ahmed M, et al. (2010) Structural conversion of neurotoxic amyloid-$\beta_{(1-42)}$ oligomers to fibrils. *Nat Struct Mol Biol* 17:561–567.
18. Klein WL, Krafft GA, Finch CE (2001) Targeting small Abeta oligomers: The solution to an Alzheimer's disease conundrum? *Trends Neurosci* 24:219–224.
19. Sakono M, Zako T (2010) Amyloid oligomers: Formation and toxicity of Abeta oligomers. *FEBS J* 277:1348–1358.
20. Zahs KR, Ashe KH (2013) β-Amyloid oligomers in aging and Alzheimer's disease. *Front Aging Neurosci* 5:28.
21. Kayed R, et al. (2003) Common structure of soluble amyloid oligomers implies common mechanism of pathogenesis. *Science* 300:486–489.
22. Tycko R (2004) Progress towards a molecular-level structural understanding of amyloid fibrils. *Curr Opin Struct Biol* 14:96–103.
23. Kirschner DA, Abraham C, Selkoe DJ (1986) X-ray diffraction from intraneuronal paired helical filaments and extraneuronal amyloid fibers in Alzheimer disease indicates cross-β conformation. *Proc Natl Acad Sci USA* 83:503–507.
24. Lührs T, et al. (2005) 3D structure of Alzheimer's amyloid-β(1-42) fibrils. *Proc Natl Acad Sci USA* 102:17342–17347.
25. Balbach JJ, et al. (2002) Supramolecular structure in full-length Alzheimer's β-amyloid fibrils: Evidence for a parallel β-sheet organization from solid-state nuclear magnetic resonance. *Biophys J* 83:1205–1216.
26. Armen RS, DeMarco ML, Alonso DO, Daggett V (2004) Pauling and Corey's α-pleated sheet structure may define the prefibrillar amyloidogenic intermediate in amyloid disease. *Proc Natl Acad Sci USA* 101:11622–11627.
27. Armen RS, Alonso DO, Daggett V (2004) Anatomy of an amyloidogenic intermediate: Conversion of β-sheet to α-sheet structure in transthyretin at acidic pH. *Structure* 12: 1847–1863.
28. Daggett V (2006) α-sheet: The toxic conformer in amyloid diseases? *Acc Chem Res* 39: 594–602.
29. Maris NL, Shea D, Bleem A, Bryers JD, Daggett V (2018) Chemical and physical variability in structural isomers of an L/D α-sheet peptide designed to inhibit amyloidogenesis. *Biochemistry* 57:507–510.
30. Linse S (2017) Monomer-dependent secondary nucleation in amyloid formation. *Biophys Rev* 9:329–338.
31. Luo J, Wärmländer SK, Gräslund A, Abrahams JP (2014) Alzheimer peptides aggregate into transient nanoglobules that nucleate fibrils. *Biochemistry* 53:6302–6308.
32. Lesné S, et al. (2006) A specific amyloid-beta protein assembly in the brain impairs memory. *Nature* 440:352–357.
33. Lesné SE, et al. (2013) Brain amyloid-β oligomers in ageing and Alzheimer's disease. *Brain* 136:1383–1398.
34. Lesné S, Kotilinek L, Ashe KH (2008) Plaque-bearing mice with reduced levels of oligomeric amyloid-beta assemblies have intact memory function. *Neuroscience* 151: 745–749.
35. Frydman-Marom A, et al. (2009) Cognitive-performance recovery of Alzheimer's disease model mice by modulation of early soluble amyloidal assemblies. *Angew Chem Int Ed Engl* 48:1981–1986.
36. Bitan G, et al. (2003) Amyloid beta-protein (Abeta) assembly: Abeta 40 and Abeta 42 oligomerize through distinct pathways. *Proc Natl Acad Sci USA* 100:330–335.
37. Bitan G, Fradinger EA, Spring SM, Teplow DB (2005) Neurotoxic protein oligomers: What you see is not always what you get. *Amyloid* 12:88–95.
38. Hopping G, et al. (2014) Designed α-sheet peptides inhibit amyloid formation by targeting toxic oligomers. *eLife* 3:e01681.
39. Kellock J, Hopping G, Caughey B, Daggett V (2016) Peptides composed of alternating L- and D-amino acids inhibit amyloidogenesis in three distinct amyloid systems independent of sequence. *J Mol Biol* 428:2317–2328.
40. Bleem A, Francisco R, Bryers JD, Daggett V (2017) Designed α-sheet peptides suppress amyloid formation in *Staphylococcus aureus* biofilms. *NPJ Biofilms Microbiomes* 3:16.
41. Breydo L, et al. (2016) Structural differences between amyloid beta oligomers. *Biochem Biophys Res Commun* 477:700–705.
42. Huang THJ, et al. (2000) Structural studies of soluble oligomers of the Alzheimer beta-amyloid peptide. *J Mol Biol* 297:73–87.
43. Torii H (2008) Amide I infrared spectral features characteristic of some untypical conformations appearing in the structures suggested for amyloids. *J Phys Chem B* 112: 8737–8743.
44. Zandomeneghi G, Krebs MR, McCammon MG, Fändrich M (2004) FTIR reveals structural differences between native β-sheet proteins and amyloid fibrils. *Protein Sci* 13: 3314–3321.
45. Hilaire MR, Ding B, Mukherjee D, Chen J, Gai F (2018) Possible existence of α-sheets in the amyloid fibrils formed by a $TTR_{105-115}$ mutant. *J Am Chem Soc* 140:629–635.
46. Quadros A, et al. (2003) Increased TNFalpha production and Cox-2 activity in organotypic brain slice cultures from APPsw transgenic mice. *Neurosci Lett* 353:66–68.
47. Kuo YM, et al. (2000) Elevated A β and apolipoprotein E in A betaPP transgenic mice and its relationship to amyloid accumulation in Alzheimer's disease. *Mol Med* 6:430–439.
48. Luo Q, et al. (2018) A self-destructive nanosweeper that captures and clears amyloid β-peptides. *Nat Commun* 9:1802–1806.
49. Link CD, et al. (2003) Gene expression analysis in a transgenic *Caenorhabditis elegans* Alzheimer's disease model. *Neurobiol Aging* 24:397–413.
50. Perni M, et al. (2017) Delivery of native proteins into *C. elegans* using a transduction protocol based on lipid vesicles. *Sci Rep* 7:15045.
51. Drake J, Link CD, Butterfield DA (2003) Oxidative stress precedes fibrillar deposition of Alzheimer's disease amyloid beta-peptide (1-42) in a transgenic *Caenorhabditis elegans* model. *Neurobiol Aging* 24:415–420.
52. Hassan WM, Dostal V, Huemann BN, Yerg JE, Link CD (2015) Identifying Aβ-specific pathogenic mechanisms using a nematode model of Alzheimer's disease. *Neurobiol Aging* 36:857–866.

Downloaded at Palestinian Territory, occupied on December 7, 2021
www.manaraa.com